Tracer-based Separation of Advection and Dispersion from Breakthrough Curves

Charles Paradis and Rakiba Sultana
University of Wisconsin at Milwaukee
Department of Geosciences
paradisc@uwm.edu

Introduction

The characterization of advection and dispersion in the breakthrough curve of a reactive solute can help determine if additional transport mechanisms, such as sorption and decay occurred. However, the breakthrough curve of a non-reactive solute tracer is first needed to characterize advection and dispersion only. This is typically done by solving the advection-dispersion equation and fitting the breakthrough curve of the non-reactive solute tracer by adjusting groundwater velocity and the dispersion coefficient; the values of velocity and dispersion are then applied to the breakthrough curve of the reactive solute and any residuals can be fit with the appropriate reactive transport mechanisms. A simpler approach is to plot the dimensionless relative concentrations of the non-reactive and reactive solute on the same graph; thus, any differences between the two curves can be attributed to reactive transport. The method proposed here can allow for separating advection and dispersion from the breakthrough curve of a reactive solute based on data only, as opposed to model-derived fitting of groundwater velocity and the dispersion coefficient, all while preserving the true concentration, as opposed to the dimensionless relative concentration, of the reactive solute. This relatively straightforward approach allows for a rapid visual separation of advection and dispersion from solute breakthrough curves to help determine if reactive mass transport mechanisms occurred. The method proposed here also includes a quantitative measure of reactivity to help identify what solutes, if any, were subject to reactive mass transport. The quantitative measure of reactivity is based on temporal moments analyses and can also help characterize what type of reactive mass transport mechanisms likely occurred; all without the need to solve the advection-dispersion-reaction equation or transform true concentrations.

Background

The development of this method begins with an example based on a field tracer test where a non-reactive solute tracer is injected into a single well followed by sampling of groundwater from the same well to generate a breakthrough curve; this is commonly known as a push-drift test. The expected concentration of a reactive solute due to advection and dispersion during a push-drift test is given by:

$$C_e^2(t) = \left(\frac{C_m^1(t) - C_b^1}{C_i^1 - C_b^1}\right)(C_i^2 - C_b^2) + C_b^2 \quad (1)$$

where: $C_e^2(t) =$ expected concentration of reactive solute due to advection and dispersion [M/L^3], $C_m^1(t) =$ measured concentration of non-reactive solute tracer [M/L^3], $C_b^1 =$ background concentration of non-reactive solute tracer [M/L^3], $C_i^1 =$ injected concentration of non-reactive solute tracer [M/L^3], $C_b^2 =$ background concentration of reactive solute [M/L^3], and $C_i^2 =$ injected concentration of reactive solute [M/L^3].

Equation (1) assumes the following: 1) the concentrations of both solutes are equal to their injection concentrations at the end of the injection, i.e., at time equal to zero, 2) the concentrations of both solutes are equal to their background concentrations as time approaches infinity, and 3) the advective and dispersive transport of the reactive solute is no different than the non-reactive solute tracer. Therefore, any difference between the measured and expected concentrations of the reactive solute can be attributed to reactivity, such as sorption and/or decay. Equation (1) has been primarily used to visually compare the measured versus expected breakthrough curves of reactive solutes to determine if reactions occurred; although some attempts have been made to characterize rate constants. However, Equation (1) has yet to be utilized in the advection-dispersion equation to test its ability to accurately characterize the expected concentration of a reactive solute due to advection and dispersion. Nor has Equation (1) been utilized to separate advection and dispersion from the breakthrough curve of a reactive solute that can have sorption and/or decay.

The objectives of this work are as follows:

1) Test the validity of Equation (1) under known flow and transport conditions
2) Utilize Equation (1) to visually separate advection, dispersion, sorption, and/or decay
3) Utilize Equation (1) to quantitatively separate advection, dispersion, sorption, and/or decay
4) Demonstrate the applicability of Equation (1) to a field tracer study

Collectively, these objectives aim to show how to characterize reactive mass transport among a suite of solutes based on data analysis alone, without the need to solve the advection-dispersion-reaction equation or normalize true concentrations.

Objective 1: Validity of Equation (1)

Equation (1) states that the concentration of a reactive solute, due to advection and dispersion alone, can be determined from the concentration of a non-reactive solute and the influent and background concentrations of both solutes. To test the validity of Equation (1), the advection-dispersion equation was solved, subject to the appropriate initial and boundary conditions and solution method, for two solutes under various influent and background concentrations. The concentration of the second solute from the advection dispersion equation was compared to the concentration from Equation (1); the concentrations were hypothesized to be equivalent.

The one-dimensional advection-dispersion equation can be written as:

$$\frac{\partial C^k}{\partial t} = -v_x^k \frac{\partial C^k}{\partial x} + D_x^k \frac{\partial^2 C^k}{\partial x^2} \tag{2}$$

where: C^k = concentration of kth solute [M/L^3], t = time [T], x = distance [L], v_x^k = groundwater velocity of kth solute [L/T], and D_x^k = dispersion co-efficient of kth solute [L^2/T]

and:

$$D_x^k = \alpha_x^k v_x^k + D_x^{*k} \tag{3}$$

where: α_x^k = dispersivity of kth [L] and D_x^{k*} = molecular diffusion of kth solute [L^2/T]. Equation (2) can be solved subject to the following initial and boundary conditions.

Uniform concentration initial condition:

$$C^k(x, t = 0\ ) = C_b^k \tag{4}$$

Pulse influent boundary conditions at inlet:

$$C^k(x = 0, 0 < t \leq t_i\ ) = C_i^k \tag{5}$$

$$C^k(x = 0, t > t_i\ ) = C_b^k \tag{6}$$

Zero concentration flux boundary condition at outlet:

$$\frac{\partial C^k(x \to \infty, t)}{\partial t} = 0 \tag{7}$$

where: C_b^k = background concentration of kth solute [M/L^3], C_i^k = pulse influent concentration of kth solute [M/L^3], and t_i = pulse influent duration [T]. Equation (2), subject to the initial and boundary conditions in Equations (4) through (7), can be solved numerically using an explicit, upstream, finite-difference scheme as given by:

$$\frac{C_j^k(t + \Delta t) - C_j^k(t)}{\Delta t} = -v_x^k\left(\frac{C_j^k(t) - C_{j-1}^k(t)}{\Delta x}\right) + D_x^k\left(\frac{C_{j+1}^k(t) - 2C_j^k(t) + C_{j-1}^k(t)}{\Delta x^2}\right) \tag{8}$$

where: C_j^k = concentration of kth solute at jth spatial node [M/L^3], t = earlier time [T], $t + \Delta t$ = current time [T], Δt = time step [T], and Δx = node space [L]. The finite-difference operators for advection and dispersion on the right-hand side of Equation (8) can be written in shorthand, the jth notation can be implied, and Equation (8) can be re-written as:

$$\frac{C^k(t + \Delta t) - C^k(t)}{\Delta t} = FD_{ADV}C^k(t) + FD_{DSP}C^k(t) \tag{9}$$

Equation (9) can be solved for the concentration of the kth solute at the current time as given by:

$$C^k(t + \Delta t) = [FD_{ADV}C^k(t) + FD_{DSP}C^k(t)]\ \Delta t + C^k(t) \tag{10}$$

where: $FD_{ADV}C^k(t)$ = finite-difference operator for advection [M/L^3/T] and $FD_{DSP}C^k(t)$ = finite-difference operator for dispersion [M/L^3/T]. If two solutes, k=1 and k=2, are both non-reactive then their groundwater velocities and dispersion co-efficients are equivalent, as given by:

$$v_x^1 = v_x^2 \tag{11}$$

$$D_x^1 = D_x^2 \tag{12}$$

Therefore, the concentration of the second solute ($C^2(t)$), as determined by the solution to the advection-dispersion equation, via Equation (10), is equivalent to the expected concentration of the second solute ($C_e^2(t)$), as determined by the concentrations of the first solute and the background and initial concentration of the second solute, via Equation (1), thus:

$$C^2(t) = C_e^2(t) \tag{13}$$

A relatively simple computer program was written in Fortran to compute Equation (10) with the following parameters: $\Delta x = 0.01$ ft, $\Delta t = 0.001$ days, $v_x^k = 1$ ft/day, $\alpha_x^k = 0.01$ ft, $D_x^{k*} = 0.001$ ft^2/day, $t_i = 2$ days. The model contained 1001 nodes, making it 10 feet long. The concentration was observed at 4 feet for 10 days. The stability of the explicit model was conditional on its spatial and temporal discretization and the magnitudes of the velocity and the dispersion coefficient, hence the relatively fine spatial grid and temporal steps. Four cases were simulated for two solutes, with each case varying their relative influent and background concentrations to investigate all four possibilities (Table 1). The influent and background concentrations for the first solute, deemed the non-reactive solute, were either 100 or 0.1 mg/L. The influent and background concentrations for the second solute, deemed the reactive solute, were either 20 or 80 mg/L.

The breakthrough curve of the non-reactive solute showed a classic Gaussian distribution centered about 5 days with a maximum concentration of 100 mg/L and a minimum concentration of 0.1 mg/L for case 1 (Figure 1). The breakthrough curve of the reactive solute showed an inverted, yet classic, Gaussian distribution centered about 5 days with a minimum concentration of 20 mg/L and a maximum concentration of 80 mg/L for case 1 (Figure 1). The expected concentration of the reactive solute, from Equation (1), was practically identical to its concentration from Equation (10), although round-off error was notable beyond the sixth decimal place. The breakthrough curves for cases 2, 3, and 4 showed that every possible variation of influent and background concentrations of both solutes resulted in a practically identical expected concentration of the reactive solute (Figure 1). These results demonstrated that Equation (1) was valid, subject to the initial and boundary conditions, and solution method of the advection-dispersion equation. The results also showed that the concentrations of the reactive solute were identical for cases 1 and 4 and for cases 2 and 3 (Figure 1). These results indicated the only two of the four cases need be considered for further analyses: cases 1 or 4 (dilution of the reactive solute) and cases 2 or 3 (addition of the reactive solute).

Table 1 Summary of cases 1, 2, 3, and 4 in terms of possible relationships between a non-reactive and a reactive solute, C_i^1 is the influent concentration of the non-reactive solute, C_b^1 is the background concentration of the non-reactive solute, C_i^2 is the influent concentration of the reactive solute, C_b^1 is the background concentration of the reactive solute

Case	Non-Reactive Solute	Reactive Solute
1	$C_i^1 > C_b^1$	$C_i^2 < C_b^2$
2	$C_i^1 > C_b^1$	$C_i^2 > C_b^2$
3	$C_i^1 < C_b^1$	$C_i^2 > C_b^2$
4	$C_i^1 < C_b^1$	$C_i^2 < C_b^2$

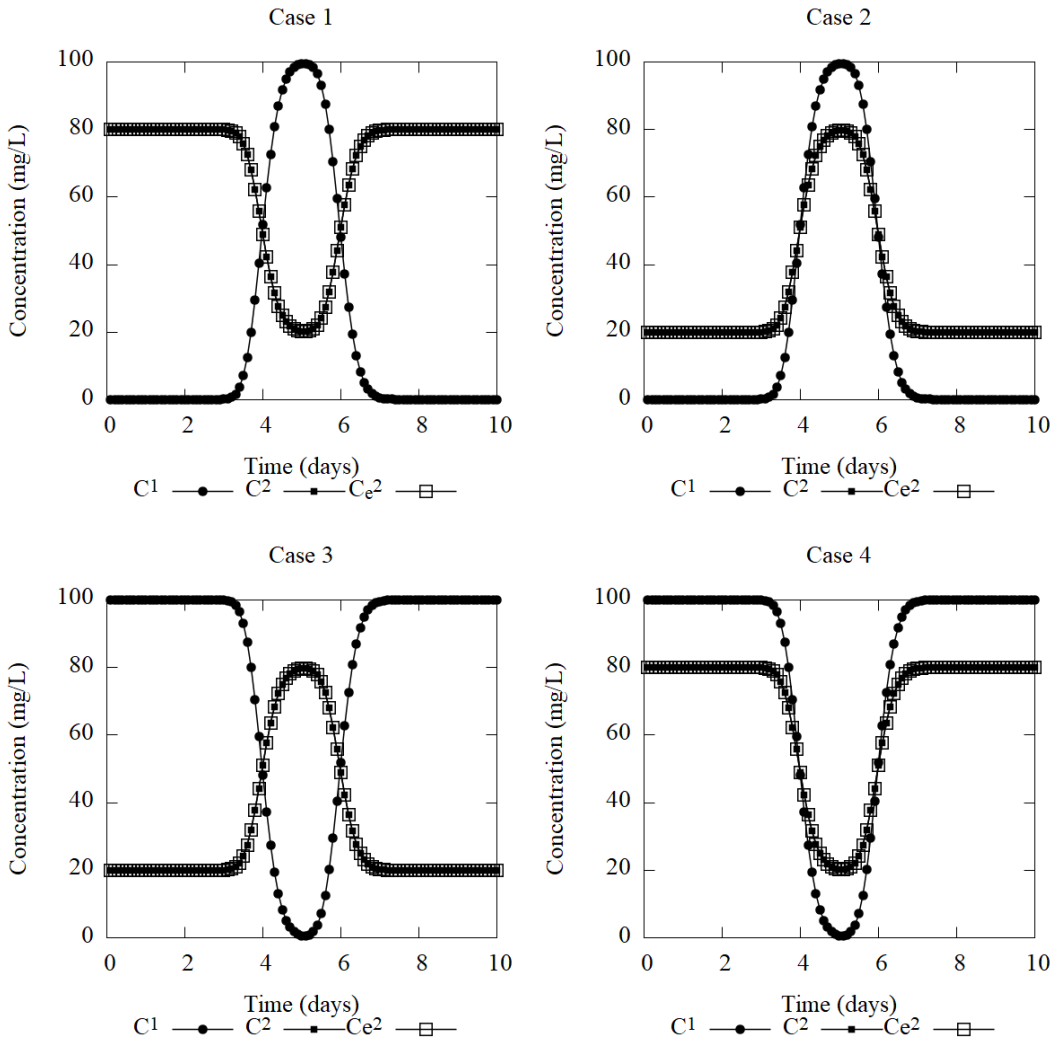

Figure 1 Model breakthrough curves of Cases 1, 2, 3, and 4 showing results from Equation (10) for the concentration of the non-reactive tracer (C^1) and the reactive tracer (C^2) and the results from Equation (1) for the expected concentration of reactive tracer (C_e^2) to test the validity of Equation (1), both Equations (10) and (1) assume advection and dispersion only

Objective 2: Visual Separation of Advection and Dispersion from Sorption and Decay

Equation (1) can accurately calculate the concentration of a reactive solute, due to advection and dispersion alone, based on the concentration of a non-reactive solute and the influent and background concentrations of both solutes. To test the ability of Equation (1) to visually separate advection and dispersion from the breakthrough curve of a reactive solute with sorption and/or decay, the advection-dispersion-reaction equation was solved, subject to the appropriate initial and boundary conditions and solution method, for two solutes under various influent and background concentrations, with the first solute subject to only advection and dispersion and the second solute additionally subject to sorption and/or decay reactions.

The concentration of the second solute due to advection and dispersion alone, from Equation (1), was compared to the concentration from the advection dispersion-reaction equation; the concentrations were hypothesized to be visually separable with sorption delaying the arrival time of the influent and decay decreasing the mass of the influent.

The advection-dispersion equation can be expanded to include reactions for the second solute as given by:

$$\frac{\partial C^2}{\partial t} = -v_x^2 \frac{\partial C^2}{\partial x} + D_x^2 \frac{\partial^2 C^2}{\partial x^2} + \sum_{n=1}^{N} RXN_n \tag{14}$$

where: RXN_n = nth reaction of the second solute [M/L^3/T]. The reaction term in Equation (14) can be explicitly written for linear-equilibrium sorption and first-order decay as given by:

$$\sum_{n=1}^{N} RXN_n = -\frac{\rho_b}{\theta} \frac{\partial \bar{C}^2}{\partial t} - \lambda C^2 \tag{15}$$

where: ρ_b = bulk density of porous media [M/L^3], θ = porosity of porous media [L^3/ L^3], $\bar{C}^2$ = concentration of second solute in the solid phase [M/M], and λ = rate constant of second solute in the aqueous phase [1/T]. Equation (15) can be substituted into Equation (14) and re-written in a finite-difference scheme as given by:

$$C^2(t + \Delta t) = [FD_{ADV} C^2(t) + FD_{DSP} C^2(t) - \lambda C^2(t)] \frac{\Delta t}{R} + C^2(t) \tag{16}$$

where: R = retention factor [dimensionless]. The first-order decay term ($\lambda C^2(t)$) in Equation (16) can be adjusted for the background concentration of the reactive solute (C_b^2) and re-written as:

$$C^2(t + \Delta t) = [FD_{ADV} C^2(t) + FD_{DSP} C^2(t) - \lambda |C^2(t) - C_b^2|] \frac{\Delta t}{R} + C^2(t) \tag{17}$$

This adjustment allows for decay to only occur if a change in the background concentration occurs, as is typically the case during a tracer test. The computer program to compute Equation (10) was expanded to compute Equation (17) and was conditionally stable on the magnitudes of the retention factor and the rate constant. Two cases were simulated for reactive solutes, with the first case of dilution and the second case of addition, much like cases 1 or 3 and cases 2 or 4 (Table 1), respectively, with each case having 4 sub-cases as follows: 1) advection and dispersion only, 2) advection, dispersion, and sorption, 3) advection, dispersion, and decay, and 4) advection, dispersion, sorption, and decay. The retention factor for sorption was 1.5 and the rate constant for decay was -0.05/day.

The separation of advection and dispersion from the breakthrough curve of a reactive solute was visually clear for both cases and their sub-cases of sorption, decay, and sorption and decay (Figure 2). Sorption resulted in delaying the arrival time of the influent (Figure 2). Decay resulted in decreasing the mass of the influent, as evident by less area underneath the breakthrough curve (Figure 2).

Combined sorption and decay resulted in both delayed arrival and decreased mass (Figure 2). These results demonstrated that Equation (1) was able to visually separate advection and dispersion from the breakthrough curve of a reactive solute, subject to the initial and boundary conditions, and solution method of the advection-dispersion-reaction equation.

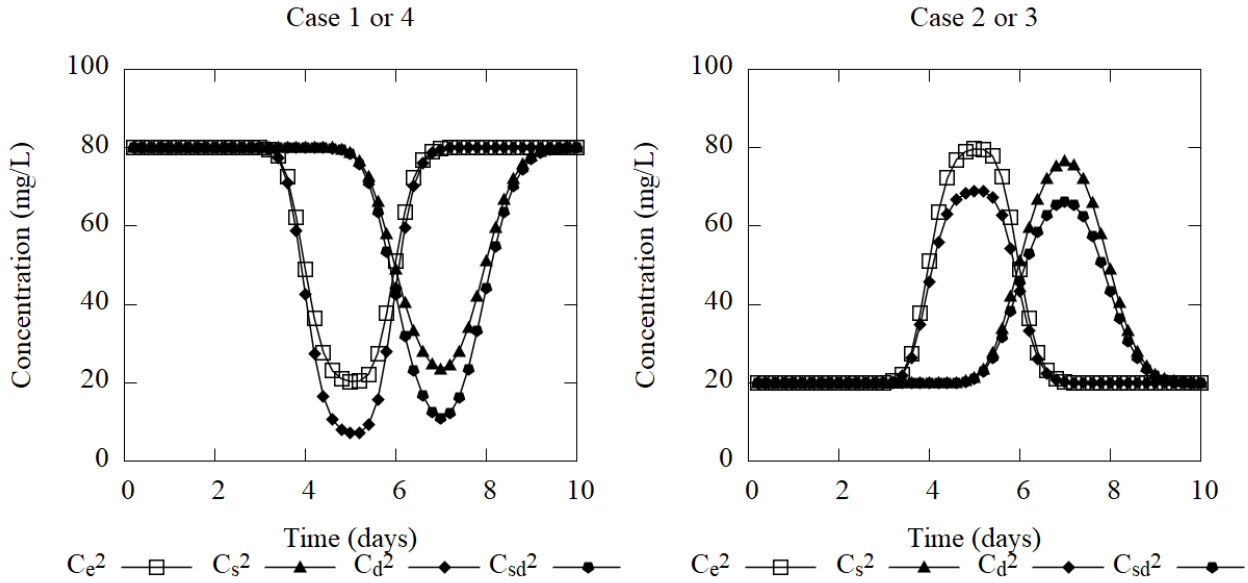

Figure 2 Model breakthrough curves of Cases 1 or 4 and 2 or 3 showing results from Equation (1) for the expected concentration of the reactive tracer (C_e^2), subject to advection and dispersion only, and the results from Equation (17) for the concentrations of reactive tracer subject to sorption (C_s^2), decay (C_d^2), and sorption and decay (C_{sd}^2)

Objective 3: Quantitative Separation of Advection and Dispersion from Sorption and Decay

The separation of advection and dispersion, via Equation (1), from the breakthrough curve of a reactive solute can be quantified using the method of temporal moments. The i[th] temporal moment for k[th] solute is given by:

$$\mu_i^k = \int_{t_o}^{t} t^i C^k dt \tag{18}$$

where: μ_i^k = i[th] temporal moment for k[th] solute [dimensionally variable], t^i = time raised to the i[th] moment [dimensionally variable], C^k = concentration of the k[th] solute [M/L^3], t_o = start time of breakthrough curve [T], t = end time of breakthrough curve [T]. The zeroth moment ($i = 0$) quantifies the area underneath the breakthrough curve. The first moment ($i = 1$), when divided by the zeroth moment ($i = 0$), is the normalized first moment, has the dimensions of time [T] and quantifies the center of mass of the solute influent. The second moment ($i = 2$), when divided by the zeroth moment ($i = 0$), is the normalized second moment, has dimensions of time squared [T^2] and quantifies the spread of the solute influent. The zeroth, normalized first, and normalized second moments are representative of solute mass, advection, and dispersion, respectively.

Equation (18), much like Equations (2) and (14), can be discretized to numerically evaluate the data of a breakthrough curve as given by:

$$\mu_i^k = \sum_{n=1}^{N-1} \left(\frac{t_{n+1}^i C_{n+1}^k + t_n^i C_n^k}{2} \right) (t_{n+1} - t_n) \tag{19}$$

where: $n =$ index of time. Equation (19) can be re-written for the case of advection and dispersion only by replacing the measured concentration of the reactive solute (C^k) with the expected concentration of the reactive solute due to advection and dispersion only (C_e^k), via Equation (1), as given by:

$$\mu_{i,e}^k = \sum_{n=1}^{N-1} \left(\frac{t_{n+1}^i C_{e,n+1}^k + t_n^i C_{e,n}^k}{2} \right) (t_{n+1} - t_n) \tag{20}$$

where: $\mu_{i,e}^k =$ ith temporal moment for kth solute due to advection and dispersion only [dimensionally variable]. Equation (19) can be divided by Equation (20) to quantify the relative zeroth moment as given by:

$$\mathrm{M}_0^k = \frac{\mu_0^k}{\mu_{0,e}^k} \tag{21}$$

where: $\mathrm{M}_0^k =$ relative zeroth moment for kth solute [dimensionless]. A relative zeroth moment greater than one indicates a net addition of solute mass to the aqueous phase, whereas a value less than one indicates a net removal; a value equal to one indicates no net addition or removal. Thus, a relative zeroth moment not equal to one indicates reactive mass transport. For moments higher than the zeroth, the relative first moment is given by:

$$\mathrm{M}_1^k = \frac{\mu_1^k / \mu_0^k}{\mu_{1,e}^k / \mu_{0,e}^k} \tag{22}$$

and the relative second moment, about the mean, is given by:

$$\mathrm{M}_2^k = \frac{\mu_2^k / \mu_0^k - \left(\mu_1^k / \mu_0^k \right)^2}{\mu_{2,e}^k / \mu_{0,e}^k - \left(\mu_{1,e}^k / \mu_{0,e}^k \right)^2} \tag{23}$$

where: $\mathrm{M}_1^k =$ relative first moment for kth solute [dimensionless] and $\mathrm{M}_2^k =$ relative second moment, about the mean, for kth solute [dimensionless].

A relative first moment not equal to one indicates a change in center of mass of the solute, e.g., a change in solute advection. A relative second moment, about the mean, not equal to one indicates a change in the spread of the solute about its center of mass, e.g., a change in solute dispersion.

The overall reactivity of a reactive solute, deemed its reactivity index, can be quantified by calculating the weighted residual sum of squares for each of the three relative moments as given by:

$$RI^k = \left\{ \left[\left(1 - \mathrm{M}_0^k\right)^2 \right] \omega_0 + \left[\left(1 - \mathrm{M}_1^k\right)^2 \right] \omega_1 + \left[\left(1 - \mathrm{M}_2^k\right)^2 \right] \omega_2 \right\} * f \qquad (24)$$

where: RI^k = reactivity index for k[th] solute [dimensionless], ω_i = weight of i[th] relative moment [dimensionless], and f = multiplication factor [dimensionless]. The weights (ω_i) in Equation (24) can range from zero to one and are chosen by the user who decides how much weight to put on reactions that affect mass (M_0), advection (M_1), and dispersion (M_2). The multiplication factor (f) in Equation (24) is chosen by the user and can typically be some factor of 10, e.g., 10, 100, 1000, etc., to avoid dealing with decimals; whole numbers are typically easier to understand and explain. In theory, a reactivity index equal to zero indicates no reactivity whereas a value greater than zero indicates reactivity. However, in practice, care must be taken to consider the inherent approximation of numerical approaches, the level of uncertainty in the data, and the importance of relative reactivity amongst k[th] solutes.

The moments and reactivity indices were calculated for model cases 1 or 4 and 2 or 3 (Figure 2) via Equations (21), (22), (23), and (24) with moment weights of one for mass, advection, and dispersion ($\omega_0 = \omega_1 = \omega_2 = 1$), and a multiplication factor (f) of 1000 (Table 2). The relative zeroth moment (M_0^2) for sorption (C_s^2) was nearly 1.00 for each case and indicated that its area under curve was no different than advection and dispersion only (Table 2). These results were expected because linear-equilibrium sorption does not result in a net change in solute mass to the aqueous phase. Both higher-order moments ($\mathrm{M}_1^2, \mathrm{M}_2^2$) were notably different than 1.00 for sorption (C_s^2) and indicated that the solute's center of mass and spread was different than advection and dispersion only (Table 1); the higher-order moments are less than 1.00 for cases 1 or 4 due to the "dip" as opposed to the "hump" for cases 2 or 3 of the solute influent, i.e., a delayed dip shifts the center of mass to an earlier time whereas a delayed hump shifts the center of mass to a later time (Figure 2). These results were expected because linear-equilibrium sorption delays the mean arrival time and increases the spreading of a solute.

The relative zeroth moment (M_0^2) for decay (C_d^2) was less than 1.00 for each case and indicated that its area under curve was less than advection and dispersion only (Table 2). These results were expected because first-order decay results in a net removal of solute mass from the aqueous phase. Both higher-order moments ($\mathrm{M}_1^2, \mathrm{M}_2^2$) were nearly 1.00 for decay (C_d^2) and indicated that the solute's center of mass and spread was not substantially different than advection and dispersion only (Table 1). These results were expected because first-order decay has relatively less effect on the mean arrival time and spreading of a solute as compared to linear-equilibrium sorption.

The relative zeroth moment (M_0^2) for sorption and decay (C_{sd}^2) were the same as those for decay (C_d^2) only for each case (Table 2). These results were expected because first-order decay results in a net change in solute mass to the aqueous phase whereas linear-equilibrium sorption does not.

Both higher-order moments (M_1^2, M_2^2) were notably different than 1.00 for sorption and decay (C_{sd}^2) and indicated that the solute's center of mass and spread was different than advection and dispersion only (Table 1). These results were expected because linear-equilibrium sorption delays the mean arrival time and increases the spreading of a solute.

The reactivity indices (RI^2) for sorption (C_s^2), decay (C_d^2), and sorption and decay (C_{sd}^2) were notably greater than zero and indicated that reactions occurred for all cases (Table 2). The reactivity indices for sorption were notably higher than for decay (Table 2) and indicated that sorption had a greater effect on the shape of breakthrough curves (Figure 2). However, the relative importance of sorption over decay was largely due to the chosen magnitudes of the retention factor ($R^2 = 1.5$) and the rate constant ($k^2 = -0.05/day$). The reactivity indices for sorption and decay were notability higher than for sorption or decay alone within each case (Table 2). These results were expected because combining sorption and decay has a greater effect on the shape of a breakthrough curve as compared to each reaction alone. Overall, these results clearly demonstrated that the method of temporal moments, as applied with Equation (1), was clearly able to quantitatively separate advection and dispersion from the breakthrough curve of a reactive solute.

Table 2 Relative moments and reactivity indices for model cases 1 or 4 and 2 or 3 (Figure 2) via Equations (21), (22), (23), and (24), M_0^2 = relative zeroth moment (mass), M_1^2 = relative first moment (advection), M_2^2 = relative second moment (dispersion), $\omega_0 = \omega_1 = \omega_2 = 1$, f=1000

	Case 1 or 4			Case 2 or 3		
Metric	C_s^2	C_d^2	C_{sd}^2	C_s^2	C_d^2	C_{sd}^2
M_0^2	0.99	0.96	0.96	1.00	0.93	0.93
M_1^2	0.93	0.99	0.91	1.15	0.99	1.13
M_2^2	0.91	1.04	0.92	1.19	1.07	1.24
RI^2 (‰)	12.8	3.03	15.9	56.8	9.06	79.0

Objective 4: Application to Field Tracer Study

The measured versus expected concentrations of field tracers and solute data were visualized for two added tracers (iodide and pentafluorobenzoate or PFB) and a suite of ten potentially reactive solutes during the drift phase of a single-well push-drift test (Figure 3); the expected concentrations due to advection and dispersion of potentially reactive solutes ($C_e^{k>1}$) were based on Equation (1) and the non-reactive added halide tracer of iodide ($C_e^{k=1}$). The measured and expected breakthrough curves of iodide were identical (Figure 3). These results were expected because iodide was chosen as the benchmark non-reactive tracer to characterize advection and dispersion only. The breakthrough curves of chloride, a non-reactive non-added halide, and PFB, a non-reactive added tracer, were nearly identical to iodide (Figure 3). These results were expected because chloride and PFB are non-reactive, meaning that their transport is largely governed by advection and dispersion only, much like iodide. The measured and expected breakthrough curves of uranium, sulfate, magnesium, and sodium were also nearly identical (Figure 3).

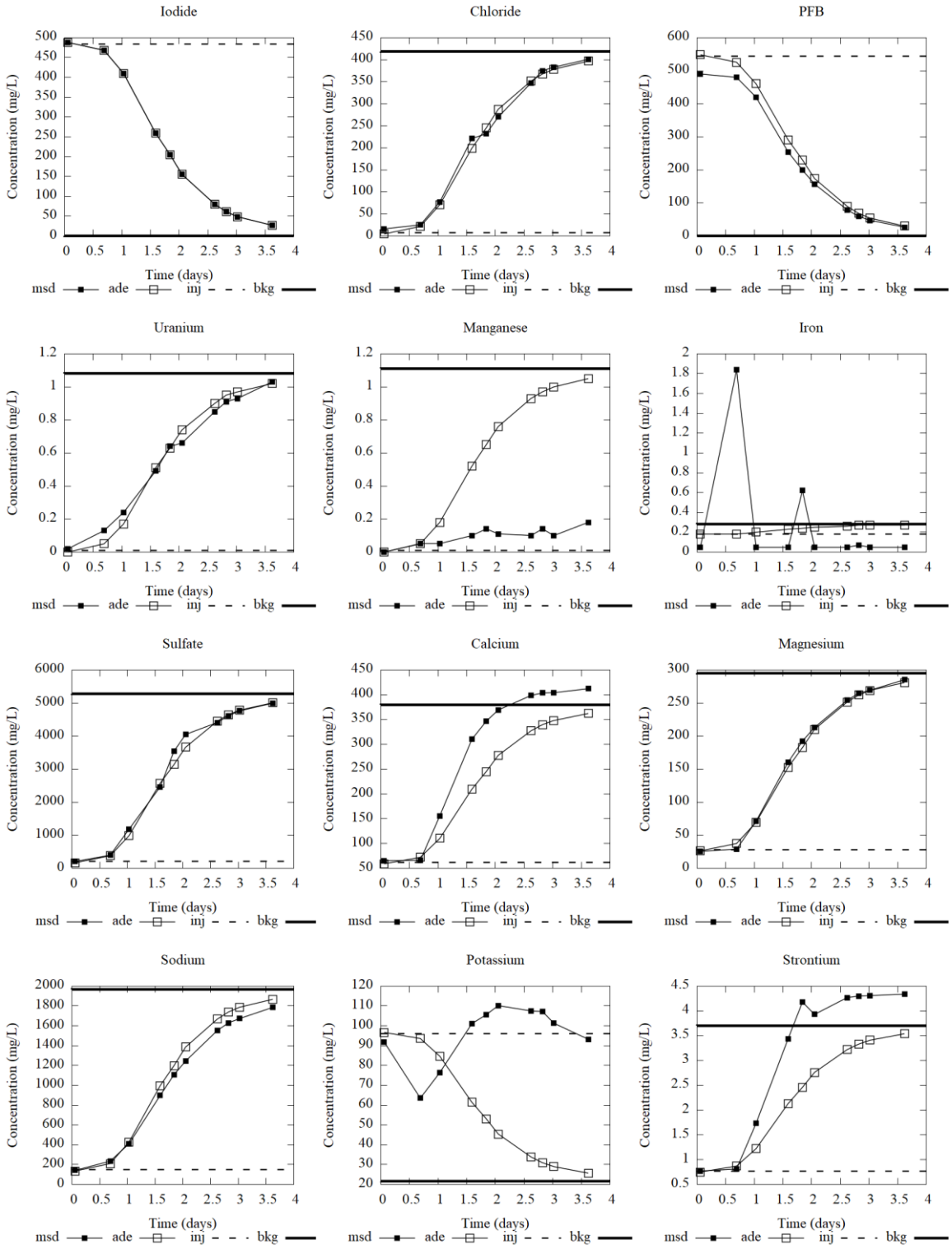

Figure 3 Field tracer and solute breakthrough curves showing measured concentration (msd ─■─), expected concentration from advection and dispersion only (adv ─□─) via Equation (1), injection concentration (inj ---), and background concentration (bkg ─)

These results indicated that uranium, sulfate, magnesium, and sodium, all of which are potentially reactive solutes, were largely non-reactive. However, the measured versus expected breakthrough curves of manganese, iron, calcium, potassium, and strontium showed considerable differences (Figure 3). These results indicated that manganese, iron, calcium, potassium, and strontium were subject to transport mechanisms in addition to advection and dispersion, i.e., reactive transport. Manganese and iron are redox sensitive solutes and tend to be soluble under reducing conditions and insoluble under oxic conditions. Therefore, it was possible that the injection fluid, if relatively oxic as compared to the background fluid, oxidized manganese and iron. This would help explain the measured concentrations of both solutes that were typically far less than expected if advection and dispersion alone were the predominant transport mechanisms (Figure 3). Calcium and potassium are base cations that can undergo cation exchange with soils. Therefore, it was possible that calcium and potassium were released from soils in exchange with one or more other cations, other than sodium and magnesium. Strontium, like calcium, is an alkaline earth metal, and may also have been subject to cation exchange. This would help explain the measured concentrations of all three solutes that were typically far higher than expected if advection and dispersion alone were the predominant transport mechanisms (Figure 3). These results demonstrated that Equation (1) was able to visually separate advection and dispersion from the breakthrough curves of a suite of potentially reactive solutes under field conditions.

The relative moments and reactivity indices were calculated for field tracer and solute data (Figure 3) via Equations (21), (22), (23), and (24) with moment weights of one for mass ($\omega_0 = 1$), advection ($\omega_1 = 1$) and dispersion ($\omega_2 = 1$), and a multiplication factor (f) of 100 (Table 3). The moments for iodide were equal to one and the reactivity index was equal to zero (Table 3). These results were expected because iodide was chosen as the benchmark non-reactive tracer to characterize advection and dispersion only. The relative moments for chloride, PFB, sulfate, magnesium, and sodium were nearly equal to one and their reactivity indices were relatively close to zero (Table 3). These results were expected because no substantial visual separation between their measured and expected breakthrough curves was observed (Figure 3). The relative moments for uranium, manganese, iron, calcium, potassium, and strontium were notably different than one and their reactivity indices were far greater than zero (Table 3). These results were expected for manganese, iron, calcium, potassium, and strontium because substantial visual separation between their measured and expected breakthrough curves were observed (Figure 3).

Table 3 Relative moments and reactivity indices for field tracer and solute data (Figure 3) via Equations (21), (22), (23), and (24), M_0^2 = relative zeroth moment (mass), M_1^2 = relative first moment (advection), M_2^2 = relative second moment (dispersion), $\omega_0 = \omega_1 = \omega_2 = 1$, f=100, **bold** values indicate reactivity

Metric	I	Cl	PFB	U	Mn	Fe	SO_4	Ca	Mg	Na	K	Sr
M_0	1.00	1.01	0.90	1.00	0.16	1.44	1.03	1.25	1.01	0.94	1.61	1.35
M_1	1.00	0.99	0.99	0.98	0.91	0.50	0.99	0.99	1.00	1.00	1.41	0.99
M_2	1.00	1.08	0.99	1.21	1.49	0.41	1.03	0.94	0.97	1.04	1.11	0.90
RI (%)	0.00	0.69	1.05	**4.50**	**95.4**	**79.1**	0.15	**6.49**	0.09	0.58	**55.6**	**13.0**

However, these results were somewhat surprising for uranium, because the visual separation of advection and dispersion appeared to be negligible (Figure 3). Upon further visual examination of the breakthrough curve (Figure 3), combined with quantitative separation (Table 3), it was clear that the reactivity of uranium was largely attributable to greater dispersion, as evident by an increased spread of concentration (Figure 3) and a relative second moment notably greater than 1 (Table 3). As for manganese, iron, calcium, potassium, and strontium, it was clear that their reactivities were commonly attributable to changes in mass (relative zeroth moments) (Table 3).

To better visualize the quantitative separation of mass, advection, and dispersion (Table 3), biplots were created to show field tracers and solutes as points with relative moments as axes (Figure 4); points that plotted away from the x=1 and y=1 coordinate indicated reactivity and points that clustered together indicated similar transport mechanisms. The biplots clearly showed that manganese, iron, and potassium were highly reactive, and that calcium and strontium were relatively less reactive yet more similar in their transport mechanisms (Figure 4); the reactivity of uranium was clearly dispersive, as compared to changes mass and advection (Figure 4). These results demonstrated that Equations (21), (22), (23), and (24) were able to quantitatively separate advection and dispersion from the breakthrough curves of a suite of potentially reactive solutes under field conditions; biplots using these equations also allowed for combined visual-quantitative separation (Figure 4).

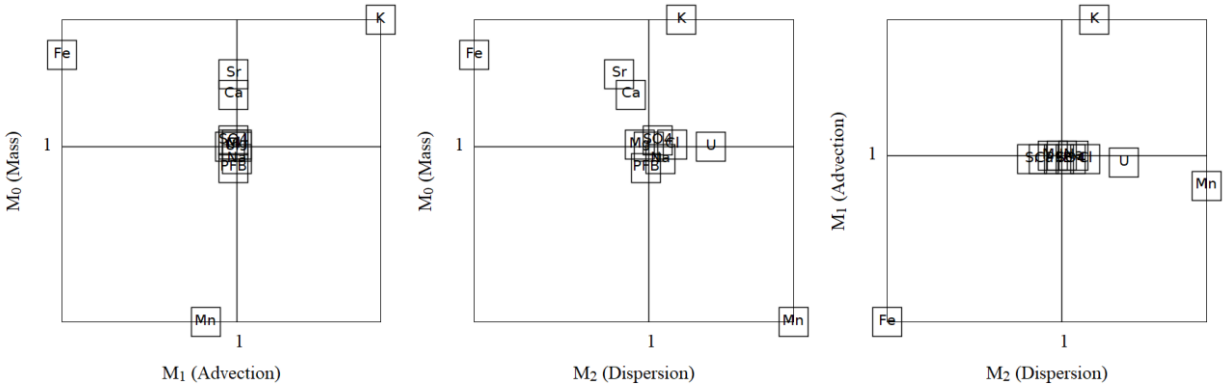

Figure 4 Biplots showing field tracers and solutes displayed as points while relative moments are displayed as axes to visualize and quantify separation of advection and dispersion, points that plot away from the x=1 and y=1 coordinate indicate reactivity, points that cluster together indicate similar transport mechanisms

Conclusions

The method proposed here allowed for visual, quantitative, and visual-quantitative separation of advection and dispersion from the breakthrough curves of variably reactive solutes based on data only, without the need to solve the advection-dispersion-reaction equation or normalize true concentrations. The method also allowed for identifying solutes with similar transport mechanisms and helped elucidate their potential mechanisms of reactive transport. The method can be used as a stand-alone analysis of tracer-based laboratory and field data or as a screening tool for future modeling efforts aimed at fitting solute breakthrough curves for advection, dispersion, and reaction parameters; the screening tool can effectively identify, cluster, and rank the reactivity of solutes and help narrow down their potential mechanisms of reactive transport.

What follows is a relatively straightforward example of applying the method to a small field tracer data set via calculations using a spreadsheet (Figure 5); these data are from the application to the field tracer study above; the non-reactive tracer was iodide (C^1) and the potentially reactive solute was manganese (C^2).

- Cells C4:D4 and C5:D5 contain the injection (C_i^k) and background (C_b^k) concentrations of iodide and the manganese.

- Cells B9:B18 contain the times that makeup the x axis of the breakthrough curve.

- Cells C9:C18 and D9:D18 contain the measured concentrations of iodide (C^1) and manganese (C^2), respectively.

- Cells E9:E18 contain the expected concentrations of manganese (C_e^2), due to advection and dispersion only, via Equation (1).

- Cells F9:F18 and G9:G18 contain the measured (C^2) and expected (C_e^2) concentrations of manganese, respectively, multiplied by time; these columns are needed to calculate the first relative moment via Equation (22).

- Cells H9:H18 and I9:I18 contain the measured (C^2) and expected (C_e^2) concentrations of manganese, respectively, multiplied by time squared; these columns are needed to calculate the second relative moment, about the mean, via Equation (23).

- Cells C21:D21, C22:D22, and C23:D23 contain the zeroth, first, and second moments of the measured (C^2) and expected (C_e^2) breakthrough curves, respectively, via Equations (19) and (20).

- Cells G21:G23 contain the relative zeroth, relative first, and relative second moment, about the mean, of the measured (C^2) and expected (C_e^2) breakthrough curves, respectively, via Equations (21), (22), and (23), respectively.

- Cell I23 contains the reactivity index of manganese via Equation (24).

	C^1	C^2
Sol.	ppm	ppm
Inj.	484.33	0.01
Bkg.	0.50	1.11

Time	C^1	C^2	C_e^2	$t*C^2$	$t*C_e^2$	t^2*C^2	$t^2*C_e^2$
days	ppm	ppm	ppm	days*ppm	days*ppm	days^2*ppm	days^2*ppm
0.06	488.00	0.00	0.00	0.00	0.00	0.00	0.00
0.69	468.00	0.05	0.05	0.03	0.03	0.02	0.02
1.03	410.00	0.05	0.18	0.05	0.18	0.05	0.19
1.59	259.00	0.10	0.52	0.16	0.83	0.25	1.32
1.84	205.00	0.14	0.65	0.26	1.19	0.47	2.18
2.05	155.00	0.11	0.76	0.23	1.56	0.46	3.19
2.62	80.00	0.10	0.93	0.26	2.43	0.69	6.38
2.82	61.00	0.14	0.97	0.39	2.74	1.11	7.73
3.02	48.20	0.10	1.00	0.30	3.02	0.91	9.13
3.62	26.70	0.18	1.05	0.65	3.80	2.36	13.77

	C^2	C_e^2
μ_0	0.32	2.03
μ_1	0.75	5.15
μ_2	1.99	14.16

	C^2
M_0	0.16
M_1	0.91
M_2	1.49

C^2
RI
95.36

Figure 5 Example spreadsheet showing the layout of calculating the expected concentration of a potentially reactive solute (C_e^2), due to advection and dispersion only, via Equation (1), and its relative moments (M_0, M_1, M_2) and reactivity index (RI) via Equations (21), (22), (23), and (24), respectively, example above was for the application to the field tracer study, the non-reactive tracer was iodide (C^1) and the potentially reactive solute was manganese (C^2), $\omega_0 = \omega_1 = \omega_2 = 1$, f=100

References

The following list of references may be useful for the reader who is interested in learning more about solute transport, tracer studies, analytical and numerical methods, computer programming, and data visualization.

Applied Studies and Technology Persistent Secondary Contaminant Sources Data Release from Field Tracer Testing Studies at the Riverton, Wyoming, Processing Site. March 2023. LMS/RSL/43015.

Chapman, Stephen J. Fortran 90/95 for scientists and engineers. New York, NY, USA: McGraw-Hill Higher Education, 2004.

Field, Malcolm S. The QTRACER2 program for tracer-breakthrough curve analysis for tracer tests in karstic aquifers and other hydrologic systems. National Center for Environmental Assessment--Washington Office, Office of Research and Development, US Environmental Protection Agency, 2002.

Goltz, Mark, and Junqi Huang. Analytical modeling of solute transport in groundwater: using models to understand the effect of natural processes on contaminant fate and transport. Vol. 1. John Wiley & Sons, 2017.

Helsel, Dennis R., et al. "Statistical methods in water resources: US Geological Survey Techniques and Methods." book 4 (2020): 458.

Hoss, Kendyl N. Mass Transport of Uranium During Recharge of Surface Water to Contaminated Groundwater. Thesis. The University of Wisconsin-Milwaukee, 2022.

Istok, Jonathan David. Push-pull tests for site characterization. Vol. 144. Springer Science & Business Media, 2012.

Janert, Philipp K. Gnuplot in action: understanding data with graphs. Simon and Schuster, 2016.

Paradis, Charles J., et al. "Improved method for estimating reaction rates during push-pull tests." Groundwater 57.2 (2019): 292-302.

Paradis, Charles J., et al. "Elucidating mobilization mechanisms of uranium during recharge of river water to contaminated groundwater." Journal of Contaminant Hydrology 251 (2022): 104076.

Stallman, Richard M. Using and porting the GNU compiler collection. Vol. 86. Boston, MA, USA: Free Software Foundation, 1999.

Van Genuchten, M. Th. Analytical solutions of the one-dimensional convective-dispersive solute transport equation. No. 1661. US Department of Agriculture, Agricultural Research Service, 1982.

Wang, Herbert F., and Mary P. Anderson. Introduction to groundwater modeling: finite difference and finite element methods. Academic Press, 1995.

Wexler, Eliezer J. Analytical solution for one-, two-, and three-dimensional solute transport in ground-water systems with uniform flow; supplemental report; source codes for computer programs and sample data sets. No. 92-78. US Geological Survey; Copies of this report can be purchased from US Geological Survey Books and Open-File Reports Section, 1992.

Zheng, Chunmiao, and P. Patrick Wang. "MT3DMS: a modular three-dimensional multispecies transport model for simulation of advection, dispersion, and chemical reactions of contaminants in groundwater systems; documentation and user's guide." (1999).